Optics Communications 369 (2016) 89–93

Contents lists available at ScienceDirect

Optics Communications

journal homepage: www.elsevier.com/locate/optcom

Utilization of monolayer MoS_2 in Bragg stacks and metamaterial structures as broadband absorbers

Bablu Mukherjee, Ergun Simsek *

Department of Electrical and Computer Engineering, School of Engineering and Applied Science, The George Washington University, Washington, D.C. 20052, USA

ARTICLE INFO

Article history:
Received 28 August 2015
Received in revised form
4 February 2016
Accepted 16 February 2016

Keywords:
Plasmonics
Metamaterials
MoS_2
TMD
Absorbers
Reflectors

ABSTRACT

We numerically study the possibility of using atomically thin transition metal dichalcogenides (TMDs) for applications requiring broadband absorption in the visible range of the electromagnetic spectrum. We demonstrate that when monolayer TMDs are positioned into a finite-period of multilayer Bragg stack geometry, they make broadband, wide-angle, almost polarization-independent absorbers. In our study, we consider molybdenum disulfide (MoS_2) and silicon dioxide (SiO_2) as semiconducting and dielectric thin film of alternate high- and low- index films, respectively. By optimizing the thickness of the SiO_2 film, we find that monolayer MoS_2 based Bragg stacks can absorb 94.7% of the incident energy in the visible (350–700 nm). Similar structures can be engineered to make perfect reflectors for saturable absorption applications. We also demonstrate that bandwidth of metamaterial absorbers can be expanded using monolayer TMDs.

1. Introduction

Absorbers have found significant interest in research as it has many applications in energy harvesting, sensing, opto-electronics, and photonics [1–20]. In 1965, Schmidt et al. demonstrated that 91% of the incident energy could be absorbed by multilayer coatings consist of metal films sandwiched between quarter-wave thick dielectric spacer layers [4]. In the following years, engineers and scientists came up with more efficient absorbers using different materials e.g. chrome [5], nickel [6], compound [7], etc. In parallel to the improvements in our micro- and nano-fabrication capabilities, different geometries (i.e. horizontal and vertical integration [8–10]) and various structures (i.e. metallic gratings [11–13], plasmonic arrays [14–17], and metamaterials [18,19]) have been studied both theoretically and experimentally to create more efficient, durable, and broadband absorbers. For example, Pérchec et al. have shown that deep rectangular metallic grooves can absorb 98% of the incident energy at the wavelength of 475 nm [11]. In [12], researchers have demonstrated that deep metallic gratings with narrow slits have ultra-broadband absorption for a moderately narrow angle range. Another report on one-dimensional (1D) grating structure demonstrates a narrow band absorption enhancement up to 8 as compared without grating structure [13]. Similarly, regular periodic arrays of metal nanoparticles demonstrate narrow absorption width [14,15] but their operation range can be increased by varying the particle size (i.e. tapered triangle arrays integrated in a metal–insulator–metal configuration is able to achieve wide-angle 88% average absorption in the range of 380–980 nm [17]; metallic multisized disk arrays show wide-angle polarization-independent broadband absorption in infrared [16]). Wang et al. reports that fabricated MoS_2 film of thickness over 30 layers on quartz glass has a saturable absorption from ~5% to ~40% in the wavelength range of ~200–2500 nm, which can be utilized as a broadband absorber [20]. They demonstrate that the induced defects during fabrication process of the film reduce the bandgap of the MoS_2, which help for saturable broadband absorption. By placing plasmonic Au nanoparticles on top of monolayer MoS_2, the average absorption can be increased from ~8% to ~41% in 400–800 nm range [21].

All of these absorbers have some advantages and disadvantages compared to each other. Some of the aforementioned absorbers are very close to the ideal case, which is ~100% efficiency, but they require advanced lithography techniques to be manufactured. Some designs might experience performance degradation in real life under extreme conditions, such as temperature and pressure. Considering its mechanical strength, atomically thin layered materials, such as graphene and transition metal dichalcogenides (TMDs), could be functional for the design of more efficient, durable, and broadband absorbers.

For this purpose, we work with molybdenum disulfide (MoS_2), which is one of the most heavily studied TMDs in the past decade [22–25]. Monolayer MoS_2 is ~0.65 nm thick and it can absorb ~25%

* Corresponding author.
E-mail address: simsek@gwu.edu (E. Simsek).

http://dx.doi.org/10.1016/j.optcom.2016.02.038
0030-4018/

of the incident energy in the near ultraviolet part of the electromagnetic spectrum. It has two prominent absorption peaks at around ~605 nm and ~660 nm due to its strongly confined excitons and spin-orbit coupling. In a very recent study [26], Kang et al. have shown that it is possible to fabricate multi-stacked monolayer MoS_2 films and the optical absorption of single, double, and triple stacks increases almost linearly with the increasing stack number.

With these recent developments, we first examine the limits of purely excitonic absorption by studying the absorptance of monolayer MoS_2 in a Bragg stack-like geometry. Bragg stacks consist of multiple layers of alternating materials with varying refractive index and they are mainly used as mirrors. In such applications, material types and their thicknesses are chosen to maximize the reflectance of the overall structure in such a way that the complex effect refractive index has a high real (n_{eff}) and a low imaginary (k_{eff}) parts. If the materials used in the Bragg stacks are very low loss materials at a chosen wavelength and if the thickness of each stack is equal to the quarter wavelength, then the constructive interference guarantees a high reflectance at that particular wavelength. However, such Bragg stacks can be engineered to maximize the absorption as well. Imagine an effective medium with n_{eff} is close to 1 (assuming the originating medium is air) and k_{eff} is very large (i.e. $k_{eff} > 2.5$). Since the reflection is mainly controlled by refractive index and loss is proportional to the extinction coefficient, such medium should be highly absorptive with a very small reflectance. In this work, we aim to design such Bragg stacks using thin TMD films, which are semiconducting materials with high absorption coefficients. The major challenge is finding the optimum dielectric spacer thickness (between TMD films) yielding the maximum average absorption for a selected wavelength range. Here we overcome this difficulty by converting this physics problem into a numerical optimization problem. We find that when SiO_2 thickness is ~106.5 nm, indeed such geometry makes a highly efficient (average absorption of ~94.7%), wide-angle, and almost polarization independent absorber for the wavelength range of 350–700 nm.

In the second part of this work, we focus on metamaterial absorbers based on metal-dielectric-metal (MDM) triple-layer structures. MDMs utilize high dielectric constant materials placed between the patterned and continuous metal layers. It is known that extremely efficient metamaterial absorbers can be made by optimizing the layer thicknesses and pattern parameters [18,19]. For example, in [18], Cao et al. have designed an MDM that shows absorptance greater than 92% over a broad wavelength range from 640 nm to 1290 nm and a wide field-of-view up to incident angle of ±40°. However, the performance of this MDM absorber dramatically degrades in the lower portion of the visible spectrum. Since TMDs have a very high absorptance in this range, when we cover MDMs with monolayer TMDs, we should be able to resolve their low absorption issue in short wavelengths and hence increase the average absorption spectrum. To verify this possibility, we numerically study the absorptance of MDMs with and without a monolayer MoS_2 sheet and we show that monolayer MoS_2 indeed increases the absorptance around 400 nm. Our study proves that the use of TMDs may lead to more efficient, ultra-broadband, wide-angle absorbers for a large range of applications including solar energy harvesting and optical data storage.

At the end, we discuss the possibility of using TMD loaded Bragg stacks as almost perfect but narrow-band reflectors, which might be useful for saturable absorber applications including mode-locking lasers [20,31,32] and pulse shapers [30].

2. Results and discussions

The optical absorptance of MoS_2/SiO_2 based multilayered Bragg stacks (Fig. 1), where each layer is represented with its refractive index (n) and thickness (d), is calculated using the transfer-matrix method (TMM) [27]. All the materials are assumed to be non-magnetic ($\mu_r = 1$). The refractive index of SiO_2 is assumed to be 1.54. Real and imaginary parts of the refractive index of monolayer MoS_2 as a function of wavelength are taken from reference [25]. The thickness of monolayer MoS_2 layer is used as 0.65 nm. Theoretical calculation (using TMM method) and reported experimental results are compared against each other to make sure that our TMM implementation are accurate enough to study these multi-scale systems, where atomically thin materials coexist with orders-of-magnitude larger structures.

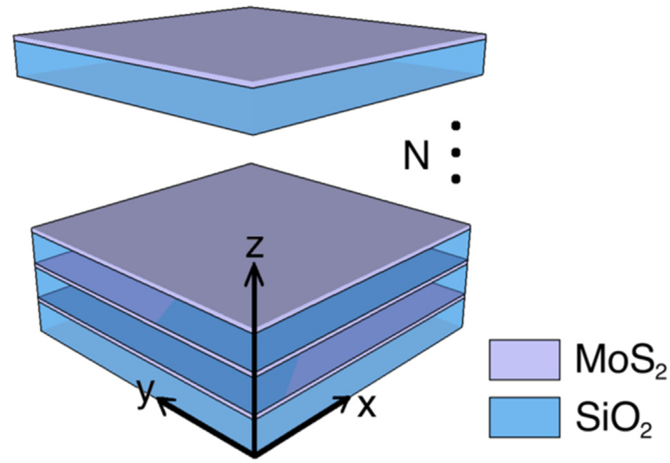

Fig. 1. Schematic representation of a finite Bragg stack consists of N units, where each unit is composed of monolayer MoS_2 and thin SiO_2 layer.

Recently Kang et al. reported experimentally the absorption spectra of vertical stacks of MoS_2/SiO_2 on fused Si substrate, which is plotted in Fig. 2b. Our calculation methodology is applied to reproduce the experimental reports [26] as shown in Fig. 2a, which match well with the reported results. The Fermi energy dependent refractive index of MoS_2 is calculated with the recipe provided in [25] assuming a Fermi energy level of 0.053 eV and room temperature. Theoretically we have obtained average absorption of ~2.6%, ~5.3% and ~7.8% from single, double and triple Bragg stack geometries, respectively. The experimental results report that the average absorption values are ~2.7%, ~5.4% and

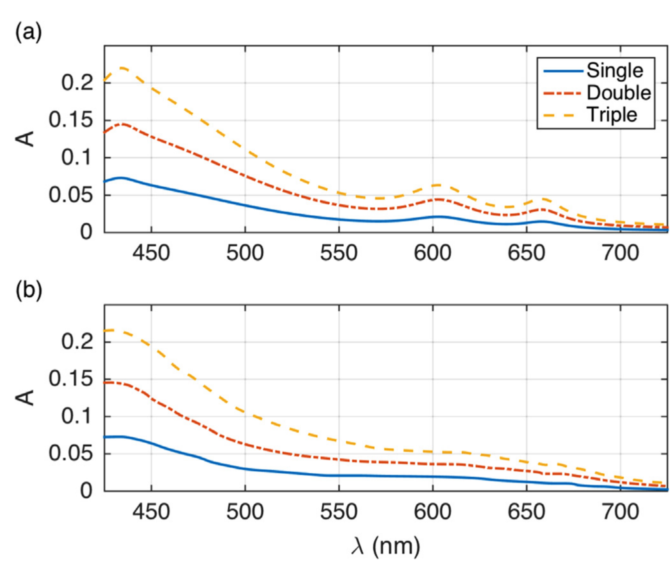

Fig. 2. (a) Optical absorption spectra calculated numerically for single-, double- and triple- unit of monolayer MoS_2/SiO_2 in wavelength range of 425–725 nm and (b) as reported experimentally in reference [26].

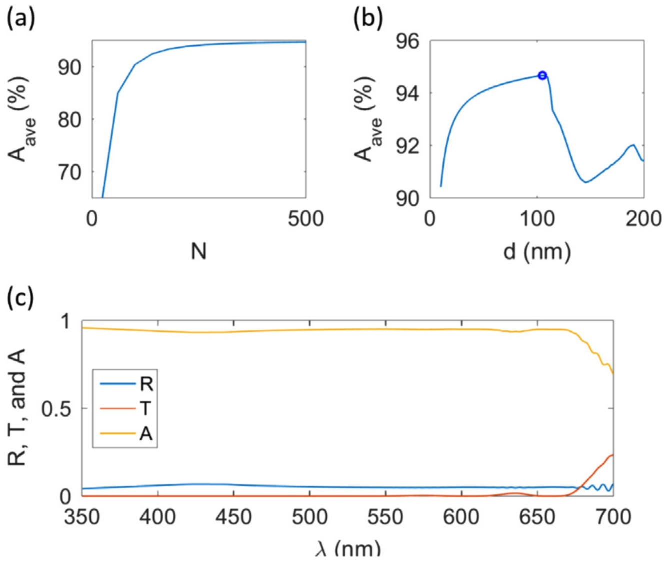

Fig. 3. (a, b) Average absorption as functions of Bragg stack number (*N*) and dielectric layer thickness (d_{SiO2}) in the wavelength range of 350–700 nm using monolayer MoS_2. (c) Reflectance (*R*), transmittance (*T*), and absorptance (*A*) spectra for 500 units of monolayer MoS_2 and 106.5 nm thick SiO_2 films.

~8.4% for single, double and triple vertical stacks, respectively, in wavelength range of 425–725 nm. Upon validation of our theoretical calculation, we analyze the Bragg stacks geometry to optimize the parameters i.e. number of stacks and SiO_2 thickness in order to achieve highest average absorption using monolayer MoS_2.

We first assume a Bragg stack with 1000 units ($N=1000$) and we change the dielectric spacer thickness (d_{SiO2}) from 10 nm to 200 nm at the step of 5 nm and calculate the average absorption (A_{ave}) at the wavelength range of 350–700 nm. This initial study shows that when the SiO_2 thickness is 106.5 nm, we obtain the highest average optical absorption of ~94.7%. Then we decrease the number of units, *N*, to 10 systematically and calculate the average absorption. As shown in Fig. 3(a), the average absorption is almost constant (94.7%), when the value of *N* is greater than or equal to 400. Also, A_{ave} is greater than 92% as long as $N \geq 200$ but it dramatically drops when *N* becomes smaller than 100. In Fig. 3(b), we plot the average absorption as a function of dielectric spacer thickness, where we also mark with a blue circle to indicate that the maximum average optical absorption (94.7%) is obtained at 106.5 nm SiO_2 thickness. Fig. 3(c) shows calculated reflectance, transmittance and absorptance as a function of wavelength for the optimum case ($N=500$ and $d_{SiO2}=106.5$ nm). Clearly, Bragg stacks composed of monolayer MoS_2 and SiO_2 spacers make broadband absorbers for normal incidence. Their performance as a function of incidence angle is examined as follows.

In Fig. 4(a) and (b), the average absorptance is plotted as a function of incidence angle for both P and S-polarizations of the irradiated plane wave, respectively. It can be observed that the average absorption is nearly independent of the incident angle for both polarizations, where the broadband response is achieved when the angle is below 60°. In addition the absorption still remains above ~80% even when the incident irradiation angles reach ~80° and ~60° for P- and S-polarized light, respectively. Thus for unpolarized light irradiation the designed Bragg stack geometry remains best absorber until the incident irradiation angle reaches ~70°.

There is no doubt that with current TMD growing capabilities, the aforementioned TMD based absorbers are very difficult to fabricate in such proposed geometry with such 500 units. However, considering the improvements in graphene synthesize methods over the last decade and novel TMD growing methods (i.e. [26] where they were able to fabricate multiple stacks), we expect that the fabrication of multilayered TMD systems integrated into alternate films will be possible in the near future.

On the other hand, a TMD based Bragg stack absorber with 500 units may be very thick for some applications, which has a theoretical limitation of ~94.7% average absorption in entire visible region (350–700 nm). As shown in Fig. 3(c), one may use much smaller number of units for slightly lower absorption efficiency. If the high efficiency is a requirement with a broad absorption range (visible to near infrared) and a thinner absorption layer, then one may consider designing hybrid absorbers by adding metamaterial absorber structures to monolayer MoS_2 to get benefit from both excitonic absorption of TMDs and localization of electromagnetic field within the dielectric interlayer of metamaterial structure. In the second part of this report, we investigate this possibility following an experimentally verified design [18].

The study [18] by Cao et al. has proposed a broadband absorber consists of an array of thin gold (Au) nanocubes separated from a continuous Au film by a phase change material GST ($Ge_2Sb_2Te_5$) layer. Their design has an absorptance of 92% or even more over a broad wavelength range from 640 nm to 1290 nm and a wide field-of-view up to incident angle of ±40°. However, the performance of their design significantly drops when $\lambda < 640$ nm. A thin film with high absorption efficiency for $\lambda < 640$ nm and very small reflectivity for $\lambda > 640$ nm can resolve this performance degradation. The utilization of atomically thin TMDs may be helpful for this purpose but their absorption is not very strong for $\lambda > 550$ nm. This is why we slightly changed their design: we

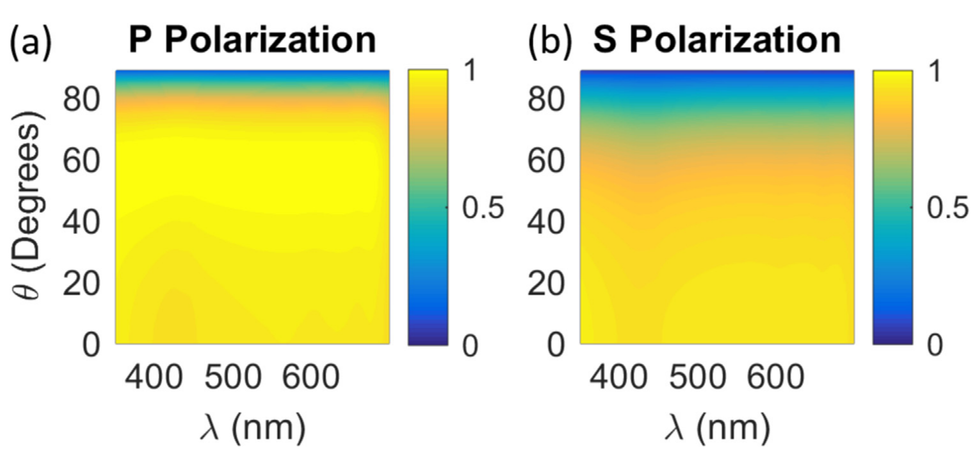

Fig. 4. Absorptance of the designed Bragg-stacks absorber as functions of incidence angle (θ) and wavelength for (a) P and (b) S-polarizations in the wavelength range of 350–700 nm.

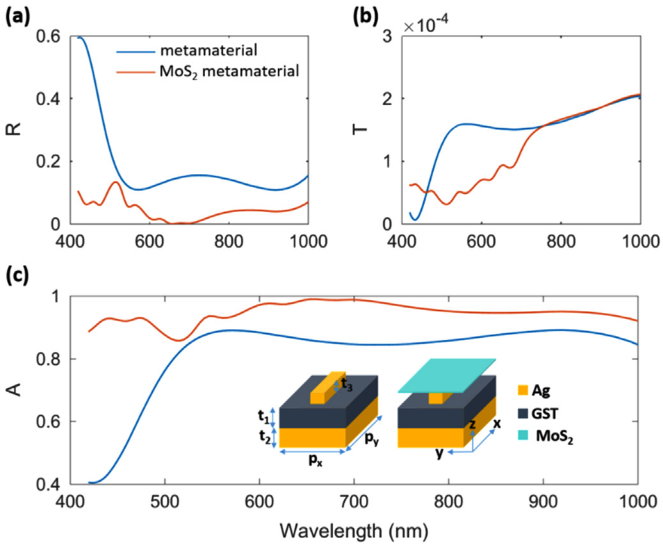

Fig. 5. (a, b, and c) Reflectance (*R*), transmittance (*T*), and absorptance (*A*) spectra of tri-layer metamaterial absorber using $Ge_2Sb_2Te_5$ dielectric film with and without monolayer MoS_2 on top of MDM metamaterial structure. Inset shows the schematic diagram of the metamaterial absorber with and without MoS_2.

assume silver (Ag) nanoparticles instead of gold (Au) nanoparticles so that we can blue-shift the plasmonic resonance. Indeed, as shown in Fig. 5 with blue line, the structure shows very strong absorptance when $\lambda > 500$ nm but its reflectivity increases when the wavelength gets closer to 400 nm. Note that here we calculate the reflectance, transmittance, and absorptance of this structure (see methods) numerically using a commercially available finite-difference time-domain (FDTD) full-wave software package, Wavenology [28]. Then we cover this metamaterial with a monolayer MoS_2 (see schematic design inset in Fig. 5c). As shown in the same figure with red lines, monolayer MoS_2 indeed help to increase the absorptance around 400 nm region. From absorptance spectra (Fig. 5c), it is calculated that the average absorption increases from ~75.4% to ~91.5% after placing monolayer MoS_2 into the metamaterial structure for the wavelength range of 400–1000 nm.

It should be noted that in [20,30–32], researchers use TMDs as a semiconducting saturable absorbing medium. They show that the nonlinear nature of this absorption involving very rich ultrafast carrier dynamics can be used for various applications ranging from mode locking [20,31,32] to pulse shaping [30]. Such nonlinear behavior requires a quantum theory treatment and cannot be simulated with a linear method as it is done in this work. However, the Bragg stacks, which we use for strong absorption purposes so far, can be utilized to maximize the reflection at particular wavelength values or ranges, as it is done in passive mode-locking devices. Assume a semiconducting saturable absorber is placed on top of a Bragg reflector, as illustrated in the inset of Fig. 6(a). The overall absorption occurring in the saturable absorber decreases with increasing excitation intensity due to the excitation of electrons from the valence band into the conduction band for photon energies just above the bandgap energy. So, such absorbers become saturated under high intensity laser pulses and allow the majority of the input energy to pass through the absorber to the Bragg stacks. If those Bragg stacks make a medium with a high effective refractive index at certain wavelengths, then they act like a mirror and reflect energy back to the saturable absorber medium, so that the light gets a second chance to be absorbed. When we lower the excitation intensity to a certain level, the saturation is broken and an increase in the absorbed energy is observed. This increase has a limit that depends on the number of electrons in the valence band of the saturable absorber medium.

In order to demonstrate its applicability, here we design two different Bragg reflectors to be used as mirrors in passive mode-locking devices operating at the wavelengths of 633 nm and 1550 nm. The first one is made of monolayer MoS_2 and 204 nm thick SiO_2 films. Fig. 6(a) shows the reflectance of this structure as a function of wavelength, which has reflectance maxima at the wavelengths of 316.5 and 633 nm. The second one is designed for telecom applications, where the wavelength of 1550 nm is the industry standard. Fig. 6(b) shows the reflectance of Bragg reflector consists of 20 nm thick MoS_2 and 285 nm thick dielectric films, where the refractive index of dielectric material is assumed to be 2.5. The inset displays the same curve zoomed in for the wavelength range of 1550–1565 nm, where the reflectance is always bigger than 95%. As a result, we can safely say that thin TMDs can be used to make Bragg mirrors for various optics and photonics applications.

Considering the fact that the other types of atomically thin TMDs (i.e. WS_2, WSe_2, $MoSe_2$, etc.) have very similar absorptance spectra, which are slightly shifted versions of each other, they also can be utilized in Bragg absorbers and reflectors with similar performances. Here, the main reasons we choose MoS_2 are that the availability of its complex refractive index for a wide range of wavelengths and our experience with it both experimentally [21,25] and theoretically [33,34].

Finally, we would like to emphasize that all the calculations are made assuming an undoped MoS_2 sample at room temperature. As

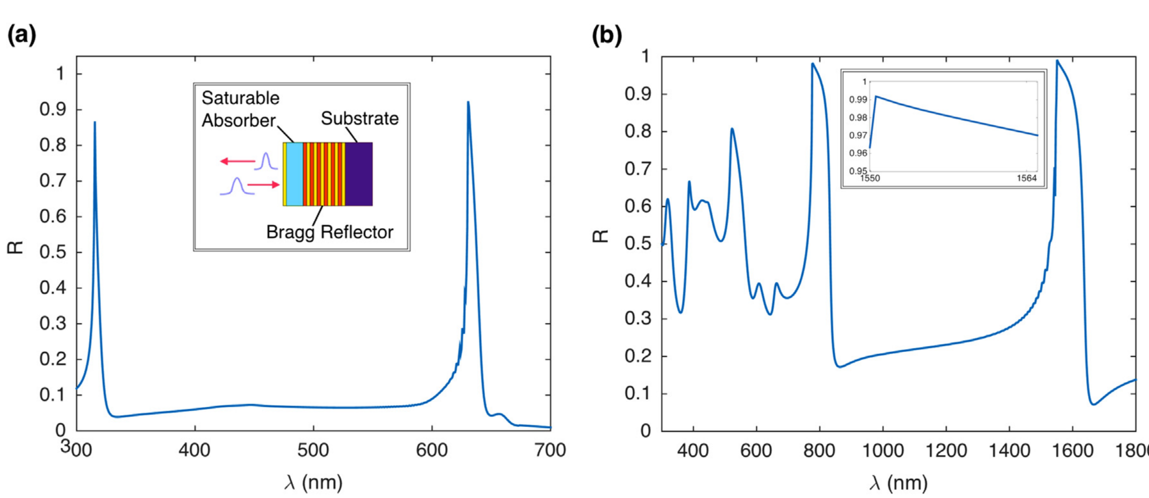

Fig. 6. Reflectance of Bragg stacks designed to be used as reflectors for (a) $\lambda = 633$ nm and (b) $\lambda = 1550$ nm.

discussed in [25], the absorptance of TMDs decreases with doping and increasing temperature. Hence any intentional or unintentional doping degrades the performance of Bragg stack based absorbers and reflectors.

3. Summary

In conclusion, monolayer MoS_2 and similar thin layer of transition metal dichalcogenides can be used in highly efficient, polarization independent and broadband absorbers in a much efficient way. By utilizing monolayer MoS_2 and optimizing the dielectric spacer thickness, the average absorptance or reflectance of the Bragg stacks can be maximized for a given range of wavelength. Theoretically, an average absorptance efficiency of ~94.7% is possible in the visible range of solar spectrum from Bragg stack geometry. Furthermore, utilization of monolayer MoS_2 in metamaterial absorbers can lead to more efficient broadband absorbers covering a full wavelength range of 400–1000 nm. For applications with longer wavelengths, thicker TMD films and dielectric materials with higher refractive indices might be required.

4. Methods

All the parameters used for the simulation results of metamaterial absorber structure are same as the ones reported in [18]. In MoS_2/metamaterial absorber structure monolayer MoS_2 is placed on top of patterned Ag film. Ag cubes (length × width × height (t_3)=140 nm × 140 nm × 100 nm) are used with a periodicity (p_x, p_y) of 300 nm along both x- and y- axes. 25 nm (t_1) GST film is used as dielectric film in the structure. 100 nm thick (t_2) Ag film is used as a back optical reflector on top of a glass as a supporting substrate. The complex dispersive refractive index of GST film is taken from [18]. The frequency-dependent permittivity of MoS_2 and Ag are taken from reference [25] and [29], respectively.

Appendix A. Supplementary material

Supplementary data associated with this article can be found in the online version at http://dx.doi.org/10.1016/j.optcom.2016.02.038.

References

[1] Y. Cui, Y. He, Y. Jin, F. Ding, L. Yang, Y. Ye, S. Zhong, Y. Lin, S. He, Laser Photon-. Rev. 8 (2014) 495–520.
[2] M.K. Hedayati, F. Faupel, M. Elbahri, Materials 7 (2014) 1221–1248.
[3] M. Lobet, M. Lard, M. Sarrazin, O. Deparis, L. Henrard, Opt. Exp. 22 (10) (2014) 12678–12690.
[4] R.N. Schmidt, K.C. Park, Appl. Opt. 4 (8) (1965) 917–925.
[5] Carl M. Lamperta, Jack Washburn, Sol. Energy Mater. 1 (1–2) (1979) 81–92.
[6] S.N. Patel, O.T. Inal, A.J. Singh, A. Scherer, Sol. Energy Mater. 11 (1985) 381–399.
[7] S. Kodama, M. Horiuchi, T. Kunii, K. Kuroda, IEEE Trans. Instrum. Meas. 39 (1) (1990) 230–232.
[8] Z.H. Jiang, S. Yun, F. Toor, D.H. Werner, T.S. Mayer, ACS Nano 5 (2011) 4641–4647.
[9] Y.Q. Ye, Y. Jin, S. He, J. Opt. Soc. Am. B 27 (2010) 498–504.
[10] X. Liu, T. Tyler, T. Starr, A.F. Starr, N.M. Jokerst, W.J. Padilla, Phys. Rev. Lett. 107 (2011) 045901–045904.
[11] J.L. Pérchec, P. Quemerais, A. Barbara, T. López-Ríos, Phys. Rev. Lett. 100 (2008) 066408–066412.
[12] Y.-L. Liao, Y. Zhao, Opt. Commun. 334 (2014) 328–331.
[13] L. Wen, F. Sun, and Q. Chen, Progress In Electromagnetics Research Symposium Proceedings, Guangzhou, China 28, 2014, pp. 1267–1271.
[14] P. Ding, G. Cai, J. Wang, J. He, C. Fan, X. Liu, E. Liang, J. Opt. 16 (2014) 065003–065010.
[15] W. Zhou, T.W. Odom, Nat. Nanotechnol. 6 (2011) 423–427.
[16] C.W. Cheng, M.N. Abbas, C.W. Chiu, K.T. Lai, M.H. Shih, Y.C. Chang, Opt. Express 20 (9) (2012) 10376–10381.
[17] G. Tagliabue, H. Eghlidi, D. Poulikakos, Nanoscale 5 (20) (2013) 9957–9962.
[18] T. Cao, C.W. Wei, R.E. Simpson, L. Zhang, M.J. Cryan, Sci. Rep. 4 (2014) 3955–3962.
[19] W. Wang, Y. Cui, Y. He, Y. Hao, Y. Lin, X. Tian, T. Ji, S. He, Opt. Lett. 39 (2) (2014) 331–334.
[20] S. Wang, H. Yu, H. Zhang, A. Wang, M. Zhao, Y. Chen, L. Mei, J. Wang, Adv. Mater. 26 (2014) 3538–3544.
[21] B. Mukherjee, E. Simsek, Plasmonics 11 (2015) 1–5.
[22] J.T. Liu, T.B. Wang, X.J. Li, N.H. Liu, J. Appl. Phys. 115 (2014) 193511–193515.
[23] X. Yang, W. Liu, M. Xiong, Y. Zhang, T. Liang, J. Yang, M. Xu, J. Ye, H. Chen, J. Mater. Chem. A 2 (2014) 14798–14806.
[24] Y. Shi, J.K. Huang, L. Jin, Y.T. Hsu, S.F. Yu, L.J. Li, H.Y. Yang, Sci. Rep. 3 (2013) 1839–1845.
[25] B. Mukherjee, K.K. Amara, G. Eda, F. Tseng, D. Gunlycke, E. Simsek, Opt. Mater. Exp. 5 (2) (2015) 447–455.
[26] K. Kang, S. Xie, L. Huang, Y. Han, P.Y. Huang, K. Fai Mak, C.J. Kim, D. Muller, J. Park, Nature 520 (2015) 656.
[27] O.S. Heavens, Optical Properties of Thin Films, Butterworth, London, 1955.
[28] Wavenology from Wave Computation Technologies, Inc., Durham, NC.
[29] E.D. Palik, G. Ghosh, Handbook of Optical Constants of Solids, Academic Press, San Diego, 1998.
[30] A. Luo, M. Liu, X. Wang, Q. Ning, W. Xu, Z. Luo, Photon-. Res. 3 (2) (2015) A69–A78.
[31] M. Zhang, R.C.T. Howe, R.I. Woodward, E.J.R. Kelleher, F. Torrisi, G. Hu, S. V. Popov, J.R. Taylor, T. Hasan, Nano Res. 8 (5) (2015) 1522–1534.
[32] J. Lin, Y. Hu, C. Chen, C. Gu, L. Xu, Opt. Express 23 (2015) 29059–29064.
[33] E. Simsek, B. Mukherjee, IOP Nanotechnol. 26 (45) (2015) 455701.
[34] F. Tseng, E. Simsek, D. Gunlycke, J. Phys.: Condens. Matter 28 (3) (2016) 034005.